Properties of water adsorbed in porous silica aerogels

A. da Silva, P. Donoso and M.A. Aegerter

Instituto de Física e Química de São Carlos, University of São Paulo, 13560 São Carlos, SP, Brazil

Silica aerogels have been prepared by hydrolysis and condensation of sols of composition TMOS–methanol–H_2O with molar ratio TMOS:H_2O = 4:1 and volume ratio TMOS:methanol = 0.2; 0.3; 0.4 and 0.6. Their true and apparent densities, BET surface area, total pore volume and pore size distribution have been systematically investigated as a function of densification heat treatment. The relaxation properties of water adsorbed on the highly reactive surface have been studied by dielectric and nuclear magnetic resonance techniques as a function of the H_2O coverage ($0 < \theta_{H_2O} < 6$) and temperature.

1. Introduction

When a wet gel is dried under supercritical conditions, the product is called an aerogel. During this process the network does not experience capillary pressure and consequently suffers little shrinkage. Aerogels have a low bulk density, a high pore volume and a large surface area.

According to Iler [1], the properties of large surface area amorphous silicates are dominated by the surface chemistry of the solid phase, which is generally terminated by hydroxyl groups. The average OH surface coverage of 100 samples of amorphous silicates, determined by Zhuravlev [2], was 4.9 OH/nm² and appeared to be independent of the form or synthesis conditions. Thermal, vacuum and chemical treatments allow dehydroxylation of the surfaces with OH groups being removed through OH condensation or chemical reaction. The dehydroxylation alters drastically the physical and chemical properties of the surface which becomes more hydrophobic and presents different ring statistics. The rehydration of a dehydroxylated surface involves adsorption followed by dissociative chemisorption. This phenomenon seems to be nucleated by strained surface acidic sites (two- or three-membered rings), and then extends to adjacent areas. Subsequent water absorption occurs preferentially on silanols formed by hydrolysis of these rings and then

extends at a much lower rate to the remaining patches of the rehydrated surface. The surface hydroxyl groups are therefore the sites where the physical adsorption of polar molecules such H_2O occurs. On a completely hydroxylated surface, H_2O molecules start to cover all the accessible isolated and H-bonded silanols. However, before the completion of a monolayer, the formation of clusters of H-bonded H_2O molecules has been observed [3], followed by multilayer condensation. Differential scanning calorimetry (DSC), dielectric relaxation spectroscopy (DRS) and nuclear magnetic resonance (NMR) have also shown that a portion of the H_2O adsorbed directly adjacent to the surface ('bound water') does not show a freezing or melting transition but remains diffusionally mobile and the remaining fraction exhibits a suppressed melting point ($T_m < 0°C$). Since the shape of the pores is not well characterized, the definition of the true thickness of the bound water layer is meaningless. Therefore, the values determined for the monolayer coverage of H_2O differ greatly among authors. This reflects the difficulty of characterization of the hydroxylated state of the surfaces and the determination of the correct cross-sectional area of H_2O molecules. A detailed review of these phenomena is given in ref. [4].

To our knowledge, the properties of water adsorbed on the surface of silica *aerogels* have

not been studied. In this paper, we report on the structural properties of silica aerogels measured during their densification and the relaxation properties of adsorbed H_2O measured by DRS and NMR techniques.

2. Experimental procedure

Silica gels were prepared by hydrolysis and condensation of sols of composition TMOS–methanol–water with molar ratio $[TMOS]:[H_2O] = 4:1$ and volume ratio $X = TMOS:methanol = 0.2; 0.3; 0.4$ and 0.6 under neutral condition. The gels are labelled M100X-N. Aerogels in form of cylinders (diameter 15 mm, length 16 cm) were obtained by hypercritical drying at $T_{max} = 310°C$, $P_{max} = 190$ bar. Samples, cut with a diamond saw, were heat treated in air under the following conditions: heating rate 2°C/min, $T = 600°C$, 700°C, 800°C, 912°C, 1000°C, 1052°C and 1100°C for different time periods. Their N_2 BET surface area, total pore volume, pore size distribution, average pore radius, and true and apparent densities have been determined using a Hg pycnometer and Micromeritics equipments Accusorb 2100E and Multivolume Pycnometer 1305.

3. Results

The nitrogen BET areas, S, are shown in fig. 1 as a function of the sintering temperatures, T_s. For unsintered samples, S is larger for lower TMOS:methanol ratios; however the temperature dependence is practically identical.

The apparent (bulk) density, ρ_b (g/cm³), of unsintered aerogels shows an opposite behavior: it remains almost constant up to $T_s = 700°C$ and then increases steadily up to $\rho_b = 2.2$ g/cm³ at full densification (fig. 2(a)). The temperature variation of the structural (true) density, ρ_s (g/cm³), measured by the pycnometer shows a complex behavior (fig. 2(a)). Similar, but less strongly marked variations have been reported for xerogels and various interrelated mechanisms have been suggested [5]. In our case the structural density of all samples starts around $\rho_s \simeq 2.0$
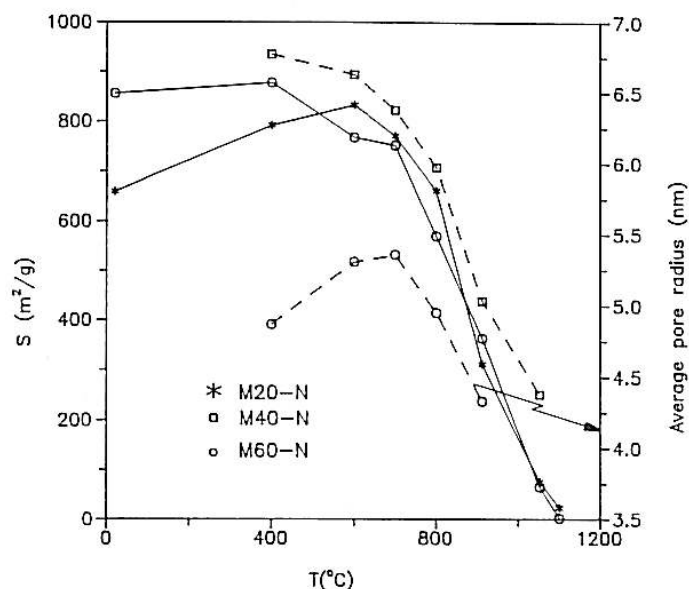

Fig. 1. Evolution of nitrogen BET surface area, S (m²/g), and mean pore radius, $r_p = 2 \ S/V_p$, where V_p is the total pore volume, as a function of the sintering temperature for aerogels M20-N, M40-N and M60-N heat treated in air for 2 h.

g/cm³; in agreement with previous results on xerogels [6,7], it increases drastically to a maximum value at $T_s = 800°C$ (for a heat treatment of 2 h) and then equilibrates at ≈ 2.2 g/cm³ when full densification is achieved. We also found that the ρ_s values depends of the time of the sintering treatment. Figure 2(b) shows a typical example for the M4O-N aerogel. The ρ_s values obtained at intermediate sintering temperatures (500–900°C) seem unrealistic; the pycnometry may not be an adequate technique for these types of materials. Considerable additional research is necessary to fully explain these behaviors.

A typical temperature evolution of the pore radius distribution and the average pore radius are shown in figs. 3 and 1 respectively for the aerogel M60-N. At low T_s, the aerogels have a broad, continuous and slowly increasing distribution of pores, peaking at a well defined radii. This sharp cut-off as well as the mean radius value depend on the sintering temperature. At higher T_s, the distribution becomes smoother.

When left in a humid atmosphere, the porous gels adsorb water. The adsorption kinetics were studied for the M60-N aerogel series, previously dried at 200°C, and placed in a 95% RH atmosphere. The time evolution of the relative ratio

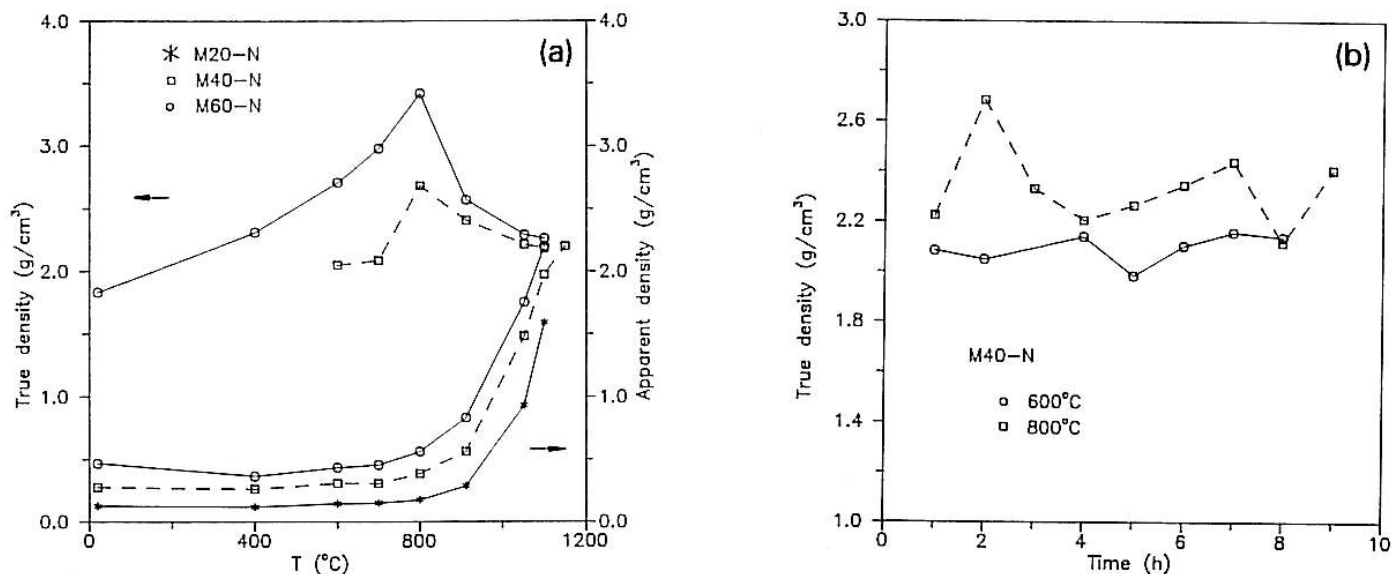Fig. 2. (a) Evolution of the structural (true) density, ρ_s (g/cm^3), and apparent density, ρ_b (g/cm^3), for various aerogels as a function of sintering temperature (heat treatment of 2 h). (b) Time evolution of the structural (true) density, ρ_s (g/cm^3), for aerogels M40-N heat treated at 600 and 800°C.

$K = [M(t) - M(0)]/[M(\infty) - M(0)]$, where M is the mass of the gel + water at the indicated times, was found identical for all gels, independent of the sintering temperature, T_s. The kinetics initially follow a $t^{1/2}$ law characteristic of a diffusion mechanism and 260 h were necessary to obtain full saturation ($K = 1$). The relative H$_2$O content, W_s (g H$_2$O/g SiO$_2$ dry), at saturation, diminishes with T_s but the relative ratio, W_s/V_p, where V_p is the total pore volume, increases with T_s, a value of 1 being only obtained for $T_s > 912$°C. This variation, also observed for xerogels [8], is probably related to the rough, fractal structure of the gel surface observed at low T_s, indicating that the adsorption behavior of H$_2$O is largely governed by pore geometry rather than surface chemistry as was thought by Iler [1].
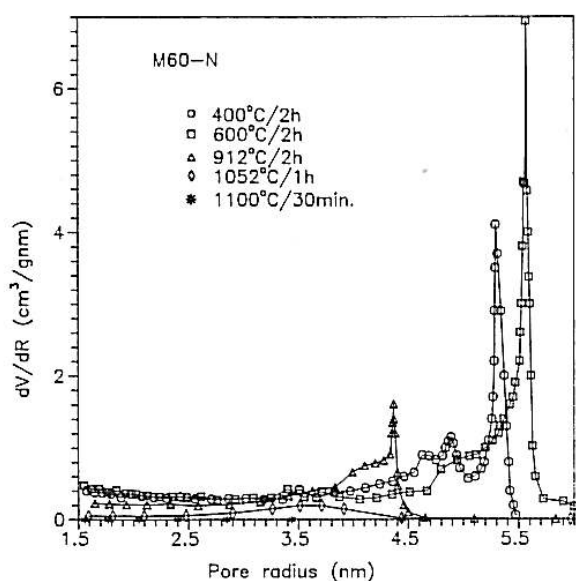
4. Nuclear magnetic resonance (NMR)

Nuclear magnetic resonance relaxation techniques are well suited to study water molecules absorbed in the vicinity of an interface. Various studies have been reported for silicate gels [9–17]. The older works [9,11] dealt with commercial products and the results were strongly affected by impurity effects. In pure silica gels, a marked decrease of the proton longitudinal and transversal relaxation time T_1 and T_2 is observed compared with the values in pure water. All the models proposed suggest that the pore fluid contains at least two separate phases: a surface phase (bound water) which has a short relaxation time and a bulk phase with a long relaxation time. These two phases are in rapid exchange. The

Fig. 3. Evolution of the pore size distribution for aerogels M60-N heat treated in air at: ○, 400°C, □, 600°C; △, 912°C; ◇, 1052°C; and *, 1100°C.

observed relaxation times and population fractions have been calculated as a function of the lifetime of the nuclei in these two phases [11–14].

The temperature dependence of the longitudinal and transverse relaxation times T_1 and T_2 of the aerogel M60-N, heat treated at 600°C for 2 h and rehydrated to different H_2O coverages, $0 \leqslant \theta_{H_2O} < 6$, has been measured using a pulse NMR spectrometer working at 24.04 MHz. T_1 was determined by the progressive saturation method [18]; the T_2 values, longer than 100 μs, were determined by spin–echo technique (excitation pulse $\pi/2 \approx 2$ μs, dead time of detector $= 12$ μs) and the faster values have been obtained directly from the free induction decay of the magnetization following a $\pi/2$ pulse. Contrary to Woessner [14], the relaxation curves exhibited only a single component whatever the temperature and water coverage.

The room temperature T_1 data are in excellent agreement with those of Hanus and Gillis [16] obtained for a silica powder used for catalysis support (Alfa Division). Using the indices 'a' to describe the bulk H_2O phase and 'b' for the bound H_2O phase, the normalized relaxation rate $R_1 = T_1^{-1}$ obs$/T_{1a}^{-1}$ increases linearly with the silica–water ratio C (fig. 4). The slope of the straight line is

$$\alpha = 2.99 \times 10^{-5} \sigma S (R_{1b}/R_{1a} - 1) = 1.43, \qquad (1)$$

where $\sigma = 9.25$ (nm^{-2}) [10–15] is the bound water molecular surface density and $S = 787$ m^2/g is the aerogel specific surface. The lower limit for the relaxation ratio T_{1b}^{-1}/T_{1a}^{-1} being 7.6, T_{1b} (bound water) is therefore $\leqslant 0.25$ s, indicating the existence of cross-relaxation between the protons in the bound phase and the surface nuclei (protons of the hydroxyl groups).

The room temperature variation of T_2 is shown in fig. 5 and clearly indicates a drastic change for water coverage around $\theta \approx 2.2$ which is believed to delimit the transition between bound and bulk water.

Three typical temperature dependences of T_1 and T_2 are shown in fig. 6 for water coverage $\theta = 3.7$, 2.8 and 0.6, respectively. When the temperature decreases, the T_1 values diminish and pass through a minimum. The data obtained with
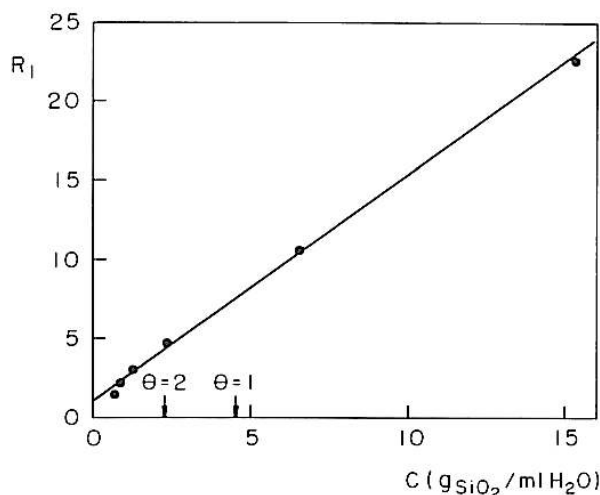

Fig. 4. Normalized relaxation rate, $R_1 = T_1^{-1}$ obs$/T_{1a}^{-1}$, measured at room temperature versus silica–water ratio C (gSiO$_2$/mlH$_2$O) for the aerogel M60-N heat treated at 600°C for 2 h. The value $T_{1a} = 0.5$ s was used to scale down the straight line to $R_1 = 1$ for $C = 0$ and corresponds to the value of pure water containing 5×10^{18} O$_2$ molecules/g H$_2$O [19]. The water coverage, θ, shown by the arrows were calculated assuming a H$_2$O molecule area of 0.108 nm^2 [10–15] ($\theta = 1$ corresponds to one monolayer).

$\theta = 3.7$ indicate a change of state (depressed freezing point) occurring at $-20°C$. This transition is not as pronounced for $\theta = 2.8$ and does not occur for $\theta = 0.6$. Moreover, the shift of the
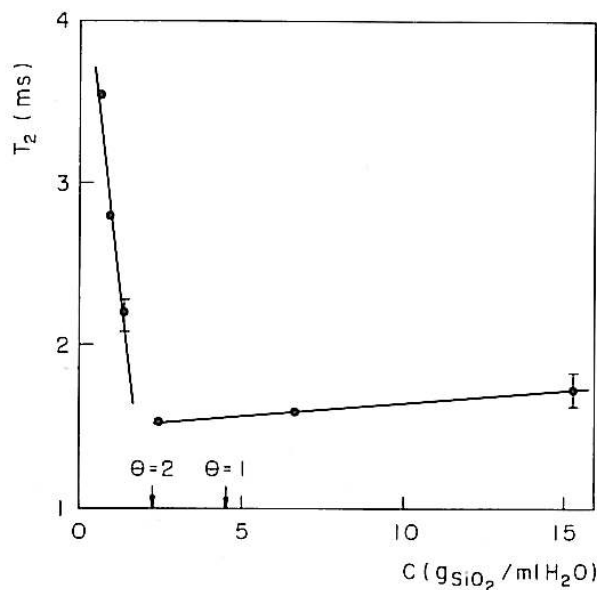

Fig. 5. Room temperature variation of the transverse relaxation time, T_2, of the aerogel M60-N versus the silica–water ratio, C (gSiO$_2$/mlH$_2$O). The arrows indicate the water coverage, θ, calculated with $S_{H_2O} = 0.108$ nm^2 [10–15].
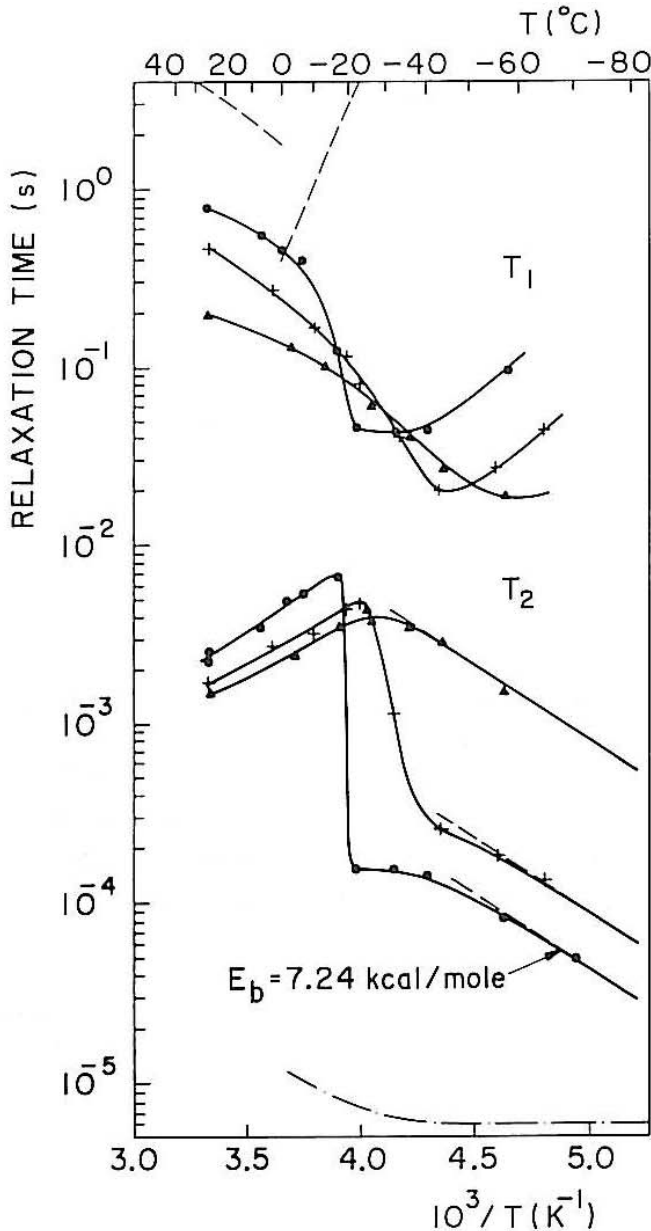
Fig. 6. Temperature dependence of T_1 and T_2 for aerogels M60-N containing: ●, $C = 1.2$ gSiO$_2$/mlH$_2$O ($\theta = 3.7$); +, $C = 1.6$ gSiO$_2$/mlH$_2$O ($\theta = 2.8$); ▲, $C = 6.6$ gSiO$_2$/mlH$_2$O ($\theta = 0.6$). ———, T_1 (= T_2) for air free water for $T > 0°$C and T_1 for single crystal hexagonal ice [19]; —·—·—, T_2 for ice [20].

minimum of T_1 toward lower temperatures when θ diminishes, indicates a decreasing water–surface interaction. The transverse relaxation data were single component at all temperatures and corroborate these results. A very sharp drop of T_2 is observed for $\theta = 3.7$. The variation is softer for $\theta = 2.8$ and does not exist at all for $\theta = 0.6$. These results are clear indications of the exis-

tence, for $\theta = 2.8$, of a bulk water phase which freezes at $T < 0°$C, the temperature shift being larger for decreasing values of θ. The low water coverage data are similar to those obtained by Woessner [13] and Michel [15]. The maximum of T_2 at $-25°$C and the subsequent decrease of T_2 at higher temperature (also observed in the two other samples) result from nuclear transfer which occurs more rapidly with increase of temperature. In all samples, the low temperature increase of T_2 with temperature has the same apparent activation energy of ≈ 7.2 kcal/mol as found by Woessner [13].

The 'freezing' process observed at low temperature does not necessarily indicate ice formation but only a reduction in molecular mobility due to the formation of a more rigid and structured layer, since the T_2 value for ice is still one order of magnitude lower.

5. Dielectric relaxation

The dielectric constant of *fused silica* measured at 20°C at audio frequencies is $\epsilon \approx 3.8$ and decreases slightly ($\Delta\epsilon'/\epsilon' \approx 0.008$) down to 4 K [21]. Dielectric losses are observed only at low temperature. A peak at $T = 27$ K was attributed to deformational losses (oscillation of bridging oxygen in nearly collinear Si–O–Si bonds) and another peak at $T < 1.3$ K was attributed to the presence of hydroxyl groups [22].

The dielectric relaxation of *silica gels* has been studied by various authors [8,23–28] and has been reviewed by Hench and West [5,29]. At room temperature, pure, dehydroxylated materials do not exhibit dielectric relaxation. When only surface silanol groups are present ($\theta_{H_2O} = 0$), a loss peak is observed at GHz frequencies, which is attributed to SiOH dipolar orientation [25,27].

Liquid water molecules have only one dipolar relaxation peak at 23.4 GHz. However, when they are adsorbed on surfaces, other relaxation frequencies appear. The bonding to the silanols causes modification in the GHz region [27]; the relaxation has been attributed both to the relative lifetimes of H-bonds formed by clusters of adsorbed water and to the rate of transfer of pro-
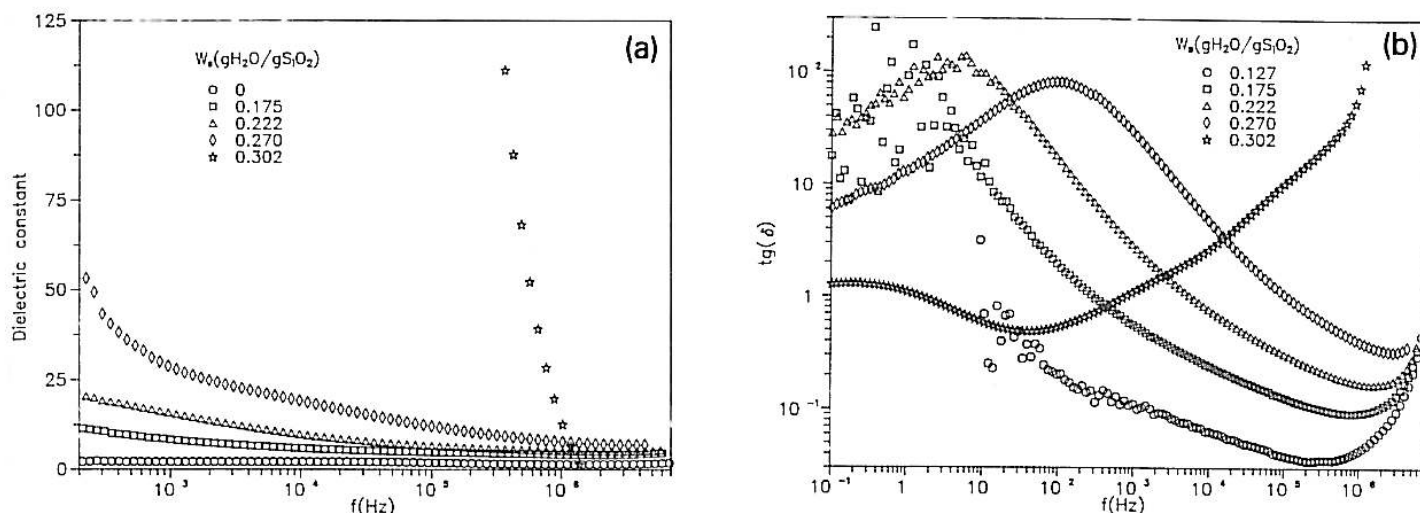
Fig. 7. Frequency dependence of (a) ϵ' and (b) tan δ measured at 25°C for an aerogel M60-N sintered at 600°C during 2 h with various amount of adsorbed water on its surface.

tons between the adjacent H-bonded water molecules adsorbed on surface SiOH groups. For $\theta_{H_2O} > 1$ [27], a second relaxation peak was observed at 14 GHz at 0°C; it is related to the formation of a free water phase.

Dielectric relaxation is also observed at audio frequencies, the frequency position of the maximum of tan θ depending strongly on water coverage and temperature [8,23,24,26,30]. The relaxation has been attributed to interfacial polarization (charge build up at the electrodes) resulting from proton conduction in the adsorbed water layer via a hopping mechanism which depends on the structure of the adsorbed water and its thickness. Direct current conductance across the terminals also causes dielectric absorption but at lower frequencies.

Adsorbed water in *aerogels* presents similar relaxation. Figure 7 shows the frequency variation of ϵ' and tan δ measured at 25°C with the aerogel M60-N for different water coverage. For $\theta = 0$, ϵ' is frequency-independent and its value is smaller than that of fused silica, reflecting the porous nature of the material [28]. For $\theta > 0$, the dielectric constant, ϵ', presents a typical dispersion behavior and its value, measured at 10^6 Hz, increases more than linearly with the H_2O content up to $W_s = 0, 30$ $gH_2O/gSiO_2$ corresponding to $\theta_{H_2O} = 1.5$ (maximum value which was possible to adsorb without breaking the aerogel). By con-

trast with xerogels [26] the loss peaks are only observed for $\theta > 1$; at lower coverage, they are located at low frequencies and are masked by dc effects even if very low applied ac signals are applied. The frequency variation versus H_2O content is shown in fig. 8 together with results
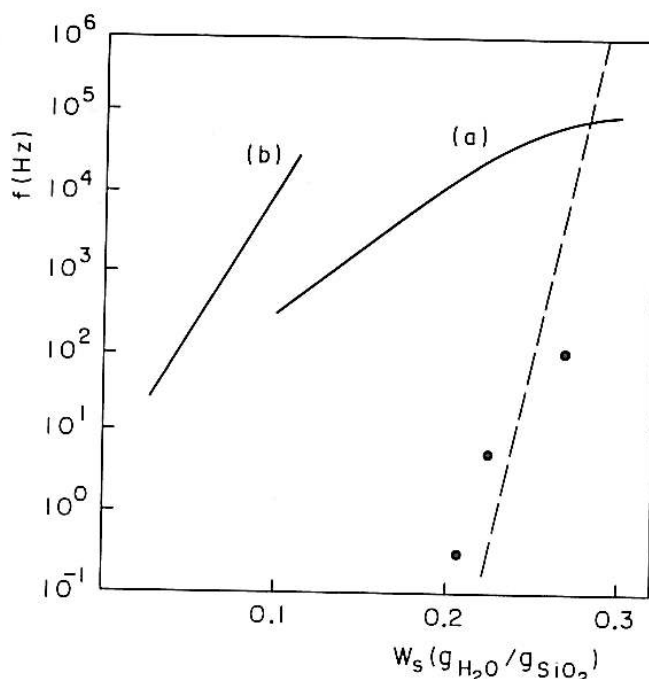

Fig. 8. Frequency dependence of the position of the maximum of the tan δ peak as a function of the amount of water adsorbed ($gH_2O/gSiO_2$). The other lines show the evolution of (a) a silica xerogel having $S = 752$ m²/g [8] and (b) a Prolabo actigel at 30°C [30].

obtained for SiO_2 xerogels [26]. The faster variation and the large shift of the peaks frequency may result from different water structure caused by the fractal nature of the aerogel surface.

6. Conclusion

A systematic study of the structural properties of silica aerogels prepared from TMOS : methanol:water sols has been presented. The main original finding is related to the drastic variation of the structural density observed during the sintering procedure. The relaxation properties of water adsorbed on the aerogel surface has been studied by dielectric relaxation spectroscopy and nuclear magnetic resonance techniques as a function of the temperature and water coverage. The overall behavior corroborates that found for silica gels or xerogels. The adsorbed water molecules belong to two different phases: H_2O molecules bonded to silanol groups and adjacent to the surface which do not show a freezing behavior and bulk H_2O molecules observed for $\theta \simeq 2$ showing a depressed freezing temperature.

References

[1] R.K. Iler, The Chemistry of Silica (Wiley, New York, 1979).
[2] L.T. Zhuravlev, Langmuir 3 (1987) 316.
[3] K. Klier and A.C. Zettlemoyer, J. Colloid Interface Sci 58 (1977) 216.
[4] C.J. Brinker and G.W. Scherer, Sol–Gel Science (Academic Press, San Diego, CA, 1990) ch. 10.
[5] L.C. Hench and J.K. West, Chem. Rev. 90 (1990) 33.
[6] F.J. Broeker, W. Heckmann, F. Fischer, M. Mielke, J. Schroeder and A. Stange, in: Aerogels, ed. J. Fricke (Springer, Heidelberg, 1986) p. 160.
[7] T. Woignier and J. Phalippou, J. Non-Cryst. Solids 93 (1987) 17.
[8] S. Wallace and L.C. Hench, in: Ultrastructure Processing of Advanced Ceramics, ed. J.D. Mackenzie and D. Ulrich (Wiley, New York, 1988) p. 873; in: Proc. 4th Ultrastructure Conf., 1989, Tucson, AZ (Wiley, New York) in press; Mater. Res. Soc. Symp. Proc. 121 (1988) 355.
[9] J.R. Zimmerman, B.G. Holmes and J.A. Lasater, J. Phys. Chem. 60 (1956) 1157.
[10] J.R. Zimmerman and W.E. Brittin, J. Phys. Chem. 61 (1957) 1328.
[11] D.E. Woessner, J. Chem. Phys. 35 (1961) 41.
[12] D.E. Woessner and J.R. Zimmerman, J. Phys. Chem. 67 (1962) 1590.
[13] D.E. Woessner, J. Chem. Phys. 39 (1963) 2783.
[14] D.E. Woessner, J. Magn. Res. 39 (1980) 297.
[15] D. Michel, Naturforsch. 22a (1967) 1751.
[16] F. Hanus and P. Gillis, J. Magn. Res. 59 (1984) 437.
[17] D.P. Gallegos, D.M. Smith and C.J. Brinker, J. Colloid Interf. Sci. 124 (1988) 186.
[18] E. Fukushima and S.B.W. Roeder, Experimental Pulse NMR (Addison Wesley, Reading, MA, 1981).
[19] J.A. Glasel, in: Water, a Comprehensive Treatise, Vol. 1, ed. F. Franks (Plenum, New York, 1972) ch. 6.
[20] N. Bloembergen, E.M. Purcell and R.V. Pound, Phys. Rev. 73 (1948) 679.
[21] S. Hunklinger and M.V. Schickfus, in: Amorphous Solids Low Temperature Properties, ed. W.A. Phillips, Springer Topics in Current Physics, Vol. 24 (Springer, Berlin, 1981) ch. 6.
[22] S.H. Mahle and R.D.Mc. Cammon, Phys. Chem. Glasses 10 (1969) 222.
[23] K. Kamiyoshi and J. Ripoche, J. Phys. Radium 19 (1958) 943.
[24] N.K. Nair and J.M. Thorp, Trans. Faraday Soc. 61 (1965) 963.
[25] L. Gengembre, J.C. Carru, A. Chapoton and B. Vandorpe, J. Chim. Phys. 76 (1979) 959.
[26] P.G. Hall, R.T. Williams and R.C.T. Slade, J. Chem. Soc. Faraday Trans. I 81 (1985) 847.
[27] I.V. Zhilenkov and E.G. Nekrasova, Russ. J. Phys. Chem. (Engl. Transl.) 54 (1980) 1503.
[28] A. da Silva, D.I. dos Santos and M.A. Aegerter, J. Non-Cryst. Solids 95&96 (1987) 1159.
[29] L.L. Hench and J.K. West, Principles of Electronic Ceramics (Wiley, New York, 1990).
[30] K. Kamiyoshi and T. Odake, Sci. Rep. Res. Instr., Tohoku Univ. 5 (1953) 271.